Electrochimica Acta 468 (2023) 143186

Contents lists available at ScienceDirect

Electrochimica Acta

journal homepage: www.journals.elsevier.com/electrochimica-acta

Ruthenium electrodeposition from non-aqueous electrolytes containing divalent ions

Federico Lissandrello [a], Roberto Bernasconi [a,*], Claudia Letizia Bianchi [b], Gianmarco Griffini [a], Luca Magagnin [a]

[a] Dipartimento di Chimica, Materiali e Ing. Chimica "Giulio Natta", Politecnico di Milano, Via Mancinelli 7, Milano 20131, Italy
[b] Dipartimento di Chimica, Università degli Studi di Milano, Via Golgi 19, Milano 20133, Italy

ARTICLE INFO

Keywords:
Electrodeposition
Ruthenium
Non-aqueous
Divalent

ABSTRACT

The electrodeposition of ruthenium from an ethylene glycol based electrolyte containing the metal in its divalent state is investigated for the first time. Ascorbic acid is used to reduce a fraction of the Ru(III) ions added to the non-aqueous solvent to Ru(II). Its effect is studied by means of UV–visible spectroscopy and cyclic voltammetry, demonstrating the presence of divalent ions and the stability of the electrolyte over time. Ruthenium coatings are deposited on gold-sputtered silicon wafers under galvanostatic conditions at various current densities and deposition times. The characterizations carried out evidence the significant purity of the ruthenium film, while the morphological analysis reveals its compact and crack-free morphology. Indeed, thicknesses up to 2.35 μm are successfully plated with no sign of delamination or cracking. The good electrical properties observed for the deposited layers validate the possible applicability of the Ru(II) containing non-aqueous electrolyte here described to the manufacturing of integrated circuits interconnects or contacts for electrical applications.

1. Introduction

Metallic ruthenium features a range of compelling properties which make it an optimal candidate material for numerous applications. For example, in the microelectronics field thin ruthenium coatings have been proposed as an alternative to copper in the metallization of interconnects in integrated circuits, where the ubiquitous downscaling is being undermined by Cu's surface scattering, which causes an increase in its resistivity at sub-50 nm sizes [1]. In contrast to copper, ruthenium exhibits good electrical conductivity and low bulk electron mean free path, which makes it less susceptible to size effects [2]. Moreover, ruthenium and its alloys have been discussed as an alternative to non-metallic barrier layers such as Ta/TaN to prevent copper diffusion in interconnects [3–5]. Not only ruthenium serves as an excellent adhesion layer for copper, but its conductive nature would enable direct Cu electrodeposition without the requirement of a seed layer [6]. Besides good conductivity, metallic ruthenium and its alloys also possess remarkable catalytic activity and durability for a variety of important reactions such as electrochemical ammonia production [7], ammonia decomposition for hydrogen production [8] and hydrocarbon electro-oxidation for fuel cells [9,10]. Finally, by capitalizing on ruthenium's electrical conductivity, stability and catalytic activity, the successful fabrication of non-enzymatic glucose sensors has been demonstrated [11,12].

Given its high price, ruthenium is rarely utilized as a standalone material, but instead used predominantly as a coating. Indeed, several vapor phase deposition methods such as PVD [13–15], CVD [15–17] and ALD [15,16,18] can be used to fabricate metallic ruthenium films. Overall, vapor phase deposition methods are relatively expensive and present their intrinsic disadvantages: PVD is a "line-of-sight" technique, where only the substrate regions directly exposed to the flow of atoms can be coated, while offering very little control on the thickness distribution. Conversely, CVD and ALD can achieve proper coating of more complex geometries, but the precursors required are often toxic and volatile. When compared to vapor phase deposition techniques, electroplating presents the best opportunities for process scalability due to its relatively low cost and complexity. The main challenge in ruthenium electrodeposition stems from its many valence states, leading to a wide variety of complexes whose electrochemical behavior is still not fully understood. Still, electroplating from aqueous electrolytes is already a well affirmed technology even at the industrial level, with sulfamate formulations containing the $[Ru_2(\mu\text{-}N)(H_2O)_2Cl_8]$ complex [19,20] also

* Corresponding author.
E-mail address: roberto.bernasconi@polimi.it (R. Bernasconi).

https://doi.org/10.1016/j.electacta.2023.143186
Received 26 July 2023; Received in revised form 8 September 2023; Accepted 8 September 2023
Available online 9 September 2023

known as μ-nitridobisaquatetrachlororuthenate. When operating at 70 °C with a pH of 2, the bath is capable of producing ruthenium coatings with a thickness up to 1.5 μm completely crack-free while maintaining a cathodic efficiency of 90% [21]. Other formulations explored in literature for ruthenium electrodeposition in aqueous systems include nitrosyl salts [22,23] or chlorides [23–25], but are not as successful. Regardless of the precursor used, deposition of high-purity coatings in aqueous environment proves to be a challenging task: although the reduction potential of ruthenium presents favorable thermodynamics [26], the sluggish kinetics of ruthenium plating result in simultaneous hydrogen evolution occurring on the surface [25,27,28]. Eventually, this leads to cracking and overall embrittlement of the deposit, thus limiting the maximum thickness achievable. Furthermore, increasing the pH to suppress hydrogen evolution is not an option in this case, as it would lead to the formation of hydrated ruthenium species [21,29].

To overcome the limitations of deposition from an aqueous environment, several alternative electrolytes have been proposed in literature, such as ionic liquids [30–32], molten salts [33] or concentrated "water-in-salt" electrolytes [34]. Despite the extremely different chemical nature of these electrolytes, they all have the common objective of suppressing or completely eliminating water secondary reactions. In addition to these examples, the successful ruthenium electrodeposition from a deep eutectic solvent based on choline chloride and ethylene glycol mixed in a 1:2 ratio [35] has been previously demonstrated. In the same study it was also observed that deposition attempts from Ru(III) precursors would lead to inadequate results and, for this reason, the possibility of introducing sulfamic acid to form the more active Ru(IV) specie was explored.

In this work, we demonstrate the use of ethylene glycol as a possible non-aqueous solvent for ruthenium electrodeposition. While ethylene glycol offers a much lower conductivity than its deep eutectic solvent counterpart, its low cost, low toxicity, and non-flammable nature make it a valuable option for the deposition of a wide variety of metals and alloys [36–40]. In order to circumvent the issues related to the plating from a (III) oxidation state, we propose a diametrically opposite approach with respect to the existing literature [35]: in place of oxidizing Ru(III) to Ru(IV), we reduce Ru(III) to Ru(II). To this extent, ascorbic acid is added to the electrolyte, leading to the formation of highly active Ru(II) species. The resulting bath yields, under galvanostatic deposition, compact and crack free metallic layers with thicknesses in excess of 2 μm.

2. Experimental section

2.1. Electrolyte characterization

Ethylene glycol (EG), $RuCl_3 \bullet xH_2O$ and ascorbic acid were purchased from Sigma-Aldrich and used without further purification. The hydration of $RuCl_3 \bullet xH_2O$ was estimated to be around 2.87 through ICP-OES (Perkin Elmer Optima 8300). Unless otherwise specified, the electrolytes were prepared by adding $RuCl_3 \bullet xH_2O$ and ascorbic acid to EG and stirred for 24 h at 80 °C in order to ensure proper dissolution of the precursors and completion of the reaction between them. UV-visible spectrophotometry was performed employing a JASCO V360. Electrolyte conductivity was measured as a function of temperature using a AMEL model 2131 conductivity probe. Karl Fischer titration was performed with a Metrohm 870 KF Titrino Plus. Finally, electrochemical characterization of the solutions was carried out by cyclic voltammetry using a Biologic VSP-300 potentiostat. The measurements were collected in a three-electrode cell, where the electrolyte was maintained at 70 °C. Glassy carbon was used as working electrode, while a platinum wire and a platinum mesh were used respectively as pseudo-reference electrode and counter electrode.

2.2. Electrodeposition of Ru coatings

Electrodeposition of ruthenium on gold-sputtered silicon wafer was carried out in galvanostatic conditions in a two-electrode cell with platinum mesh as counter electrode. Prior to the deposition, the substrates were ultrasonically cleaned in acetone for 10 min. During the deposition, the electrolyte was gently stirred and maintained at a temperature of 70 °C. Different samples were prepared by varying the current density (5 – 20 mA cm^{-2}) and deposition time (500 – 4000 s). Finally, the samples were dried under ultrapure N_2 flow, to prevent oxidation of the freshly deposited ruthenium.

2.3. Coatings characterization

SEM images were collected with a Zeiss EVO 50 EP and used to investigate coatings morphology and to estimate their thickness. Additionally, morphology results were corroborated with AFM measurements performed with a NT-MDT SOLVER PRO. XRD measurements were performed with a Philips PW1830 diffractometer using a Cu source ($K_{\alpha 1}Cu = 1.54058$ Å). XPS measurements were carried out with a Surface Science M-Probe ESCA/XPS equipped with an Al source. Finally, coatings surface and bulk resistivity was measured with a Jandel AM7 4-points probe.

3. Results and discussion

3.1. Physical and chemical characterization of the electrolytes

The addition of ascorbic acid in the 100 mM $RuCl_3$ in EG electrolyte triggered a chemical reaction, as highlighted by the change in color of the solution (Fig. 1a and b). The color shift could be observed at room temperature after days, whereas an increase in temperature led to the same change in a matter of hours instead. Consequently, all the electrolytes used in this work were stirred at 80 °C for 24 h in order to complete the reaction between ascorbic acid and $RuCl_3$.

After the reaction proceeded to completion, the water content of the electrolytes was measured by Karl Fischer titration. Considering that the main appeal of non-aqueous systems is the elimination of the undesired effects of water, ensuring that the water content is kept to a minimum is of paramount importance. The content of water was measured for the 100 mM $RuCl_3$ in EG solution with the addition of 0 mM, 200 mM, and 400 mM of ascorbic acid. The weight percentage of water for the three electrolytes was respectively 0.29 ± 0.03%, 0.52 ± 0.02% and 0.75 ± 0.02%, with a fraction of this water deriving from $RuCl_3$ hydration.

The evolution of the reaction with ascorbic acid was monitored by maintaining the solution at 50 °C and collecting UV–vis spectra as a function of time. To prevent saturation of the absorbance signal, all the tests were performed with a 1:250 dilution ratio. The results in Fig. 1c show that the base electrolyte of $RuCl_3$ in EG has a sharp absorption peak (A) at 344 nm and virtually no absorption above 500 nm. Other works based on ruthenium(III) in EG also report a similar absorption spectrum [41–43], although the actual complex associated to absorption in this region has not been properly identified yet. After the addition of 200 mM ascorbic acid in solution, the intensity of peak A decreases over time, while a second peak (B) that was previously absent, appears at 694 nm. This shift in the absorption spectra might be associated to a reduction in ruthenium's oxidation state from +3 to +2 deriving from a reaction with ascorbic acid. Indeed, it has been reported in literature that Ru(II) or mixed Ru(II)/Ru(III) solutions exhibit a blue color [44,45], a description that agrees with the solutions shown in Fig. 1a and b. Accordingly, if $RuCl_3$ is dissolved in water in presence of ascorbic acid, the result is a blue colored solution presenting a clear UV–vis absorption maximum around 812 nm (Fig. S1).

In acidic aqueous systems, it has been observed that ruthenium(III) most stable chloro complex [46], that is $[Ru^{III}Cl_2(H_2O)_4]^+$, can oxidize L-ascorbic acid while forming a Ru(II) complex according to the overall

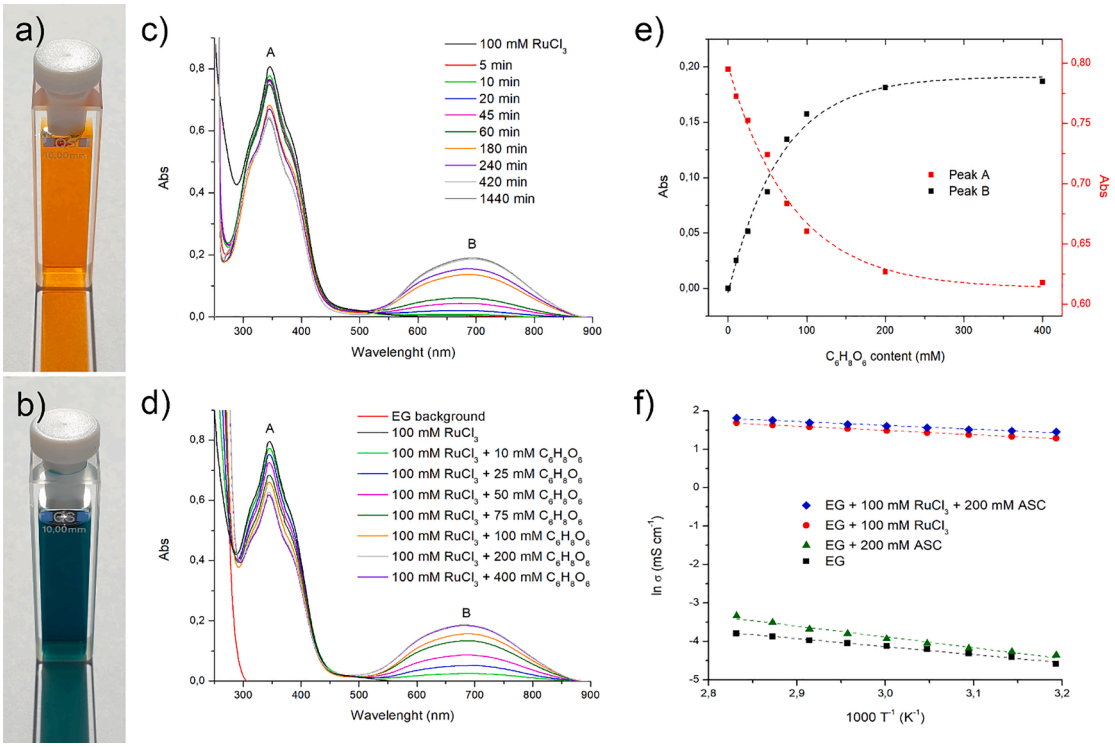

Fig. 1. (a) 100 mM $RuCl_3$ in EG after 1:25 dilution. (b) 100 mM $RuCl_3$ + 200 mM ascorbic acid in EG after 1:25 dilution. (c) Evolution of UV–vis absorption spectra of 100 mM $RuCl_3$ + 200 mM ascorbic acid in EG while heating at 50 °C. (d) UV–vis absorption spectra of 100 mM $RuCl_3$ in EG with different ascorbic acid concentrations. (e) Absorbance of the two main absorption peaks as a function of ascorbic acid concentration. (f) Conductivity of the electrolytes as a function of temperature.

reaction [47]:

$$2\left[Ru^{III}Cl_2(H_2O)_4\right]^+ + H_2Asc \rightarrow 2\left[Ru^{II}Cl_2(H_2O)_4\right] + Asc + 2H^+ \quad (1)$$

Although the reaction mechanism in EG has not been explored, it's possible that a similar process could also occur in solvents different than water. In addition to this, the decrease in the main peak absorption is typically used to monitor the reduction of the Ru(III) precursors in the synthesis of Ru(0) nanoparticles in EG through the polyol reduction method [41–43]. Keeping in mind these observations, it's extremely likely that the change in color of the solution is due to the formation of a stable Ru(II) specie. By considering a simple one-step process, it's possible to fit the time-dependent absorbance with a decreasing exponential:

$$A(t) = a\exp(-kt) + C \quad (2)$$

Where $A(t)$ is the absorbance, k is the time constant for the reaction, t is the time, while a and C are constants. The results shown in figures S2 and S3 agree fairly well with the experimental data, resulting in time constants of $k = 1.062 \bullet 10^{-4}\ s^{-1}$ for peak A and $k = 1.147 \bullet 10^{-4}\ s^{-1}$ for peak B. Interestingly, the intensities of both peak A and B stabilize for ascorbic acid contents above 200 mM (Fig. 1e), although peak A does not fully disappear. This indicates the formation of a dynamic equilibrium between ascorbic acid and ruthenium species, with the final electrolyte being a mixture of Ru(III) and Ru(II). Indeed, by exploiting the Lamber-Beer law, it's possible to estimate the fraction of Ru(II) in the system. In a dilute solution the concentration of a specie is correlated to its absorbance peak according to:

$$A = \varepsilon_\lambda\ l\ M \quad (3)$$

Where ε_λ is the molar extinction coefficient, l is the optical path and M is the molarity of the solution. The molar extinction coefficient for Ru(III) was estimated to be 1999.13 ± 15.73 $M^{-1}\ cm^{-1}$ from a three-point calibration by considering the absorbance of peak A of $RuCl_3$ solutions in EG at different concentrations. Furthermore, the concentration of Ru (II) species can be calculated by considering that all the Ru(III) reacting with ascorbic acid is converted to Ru(II):

$$[Ru(II)] = [Ru_{total}] - [Ru(III)] \quad (4)$$

By coupling Eqs. (3) and (4) it's possible to quantify the amount of Ru(II)/Ru(III) in solution as a function of time and ascorbic acid concentration (Figs. S4 and S5). From this analysis, the concentration of Ru (II) in the 100 mM $RuCl_3$ and 200 mM ascorbic acid electrolyte was estimated to be 21.59 mM.

It is worth mentioning that the one-reaction hypothesis might also be too simplistic. For example, in the case of the reduction of *cis*-dichloridobispicolinatoruthenate(III) ion by ascorbic acid in aqueous environment, the reversible electron transfer in the proposed reaction mechanism interferes with the progress of the reaction itself, with the data being more correctly interpreted by a three-exponential function [48]. Nevertheless, the complete characterization of the reduction mechanism in EG goes beyond the scope of this work. Finally, it's known that both EG and ascorbic acid are capable of reducing Ru(III) by themselves; however, ruthenium reduction in EG requires extremely high temperatures and proceeds until the metallic state, while Ru(II) species formed by reactions with ascorbic acid in aqueous environments are short lived, as they tend to be oxidized back to Ru(III) when exposed to molecular oxygen [49,50]. In the case of the 100 mM $RuCl_3$ + 200 mM ascorbic acid electrolyte, no significant changes in the absorption spectra were observed even after 6 months (Fig. S6), thus it's plausible that while ascorbic acid is directly responsible for the Ru(III) reduction, EG is also creating a sufficiently protective environment that prevents the backward reaction from occurring.

Fig. 1f shows the dependence of the electrolyte conductivity from temperature. Being a non-dissociated diol, pure EG exhibits extremely low conductivity at any given temperature, highlighting one of the main

drawbacks of this system when compared to aqueous electrolytes or ionic liquids. In general, it can be expected that the major contribution to the conductivity of EG-based electrolytes derives from the dissolution and dissociation of metal salts which introduce ions in the solution [36]. With the addition of $RuCl_3$ in solution, the conductivity does indeed increase to values between 4.27 and 6.16 mS cm^{-1}, which are suitable for electrodeposition applications. Interestingly, the addition of ascorbic acid does not provide a significant contribution to the ionic conductivity, suggesting that the molecule is hardly dissociating in EG.

3.2. Electrochemical characterization of the electrolytes

Cyclic voltammetry was performed to assess the electrochemical behavior of the EG electrolytes as well as to investigate the effect of ascorbic acid concentration.

Platinum wire was chosen as a pseudo-reference electrode for the tests since the temperature of the electrolyte (70 °C), along with the non-aqueous nature of EG, restricts the use of traditional reference electrodes [51,52]. Figs. 2a and b show the differences in cyclic voltammograms of the EG + 100 mM $RuCl_3$ electrolyte in absence or presence of 200 mM ascorbic acid. The cyclic voltammograms clearly evidence the wide electrochemical window of EG-based electrolytes which is around 2 V for this study, similar to what is reported in literature [53]. In both curves a reduction current appears as the potential is shifted towards cathodic values (Ru_{red}). The potential at which this feature appears shifts from around −0.50 V vs Pt to −0.35 V vs Pt when 200 mM of ascorbic acid are introduced in the electrolyte. Considering that this feature is also present in the curve without ascorbic acid, it's highly unlikely that it could be associated to a reduction to a metallic state. Instead, a possible explanation could be the formation of Ru complexes with valence states higher than 0 [35], with the shift being caused by the change in the solvation shell of ruthenium ions in presence of ascorbic acid. Additionally, a new reduction peak ($Ru_{(IV)red}$) appears in the second cathodic scan that was previously absent. This feature could instead be attributed to reduction of ruthenium species with higher valence states formed during the anodic scan [27]. The effect of the concentration of ascorbic acid is further highlighted in Fig. 2c and d, showing respectively the changes in the cathodic and anodic branch of the cyclic voltammetry. As anticipated, the main reduction peak shifts towards more positive values as the concentration of ascorbic acid is increased, eventually stabilizing above 100 mM. Perhaps the most striking difference between the two curves is the appearance of an oxidation peak (Asc_{ox}) with an onset around +0.2 V vs Pt in presence of ascorbic acid. To better understand the origin of this peak, two additional cyclic voltammetries were performed on the EG and EG + 200 mM ascorbic acid electrolytes. In this case the 100 mM $RuCl_3$ was replaced with 1 M NaCl to provide enough conductivity. The cyclic voltammetries in Fig. S7 show a clear oxidation peak starting at +0.6 V vs Pt when ascorbic acid is added to EG. Considering the absence of ruthenium in solution, this feature probably belongs to ascorbic acid oxidation. Ultimately, we believe that Asc_{ox} and the peak shown in Fig. S7 are fundamentally the same reaction despite the large difference in the onset potential. In fact, the reduced overpotential for ascorbic acid oxidation in Fig. 2d could be explained by considering the deposition of metallic Ru during the cathodic scan which would dramatically increase the activity of the glassy carbon substrate.

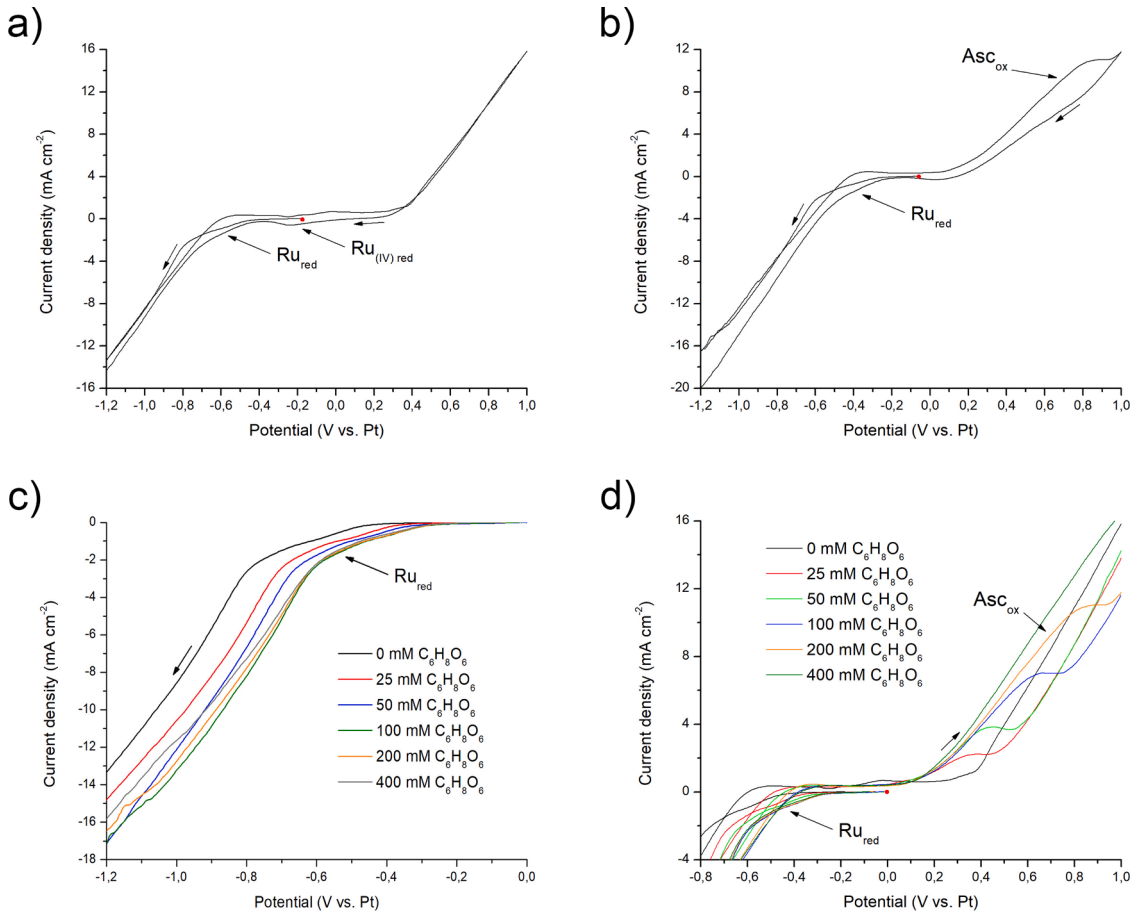

Fig. 2. Cyclic voltammetries obtained at 10 mV s^{-1} of the EG + $RuCl_3$ solutions. (a) Cyclic voltammogram of EG + 100 mM $RuCl_3$ without ascorbic acid. (b) Cyclic voltammogram of EG + 100 mM $RuCl_3$ + 200 mM ascorbic acid. (c) Zoom-in of the cathodic branch of cyclic voltammetries at various ascorbic acid concentrations. (d) Zoom-in of the Asc_{ox} peaks of cyclic voltammetries at various ascorbic acid concentrations.

3.3. Ruthenium galvanostatic electrodeposition

Metallic ruthenium deposits were obtained on gold-sputtered silicon wafers under galvanostatic conditions. The electrolyte used for the deposition contained 100 mM $RuCl_3$ + 200 mM ascorbic acid and was maintained at 70 °C during the whole process. Fig. 3a–h show SEM images and AFM measurements on selected areas of samples obtained at 5 mA cm^{-2} for various deposition times (500 s, 1000s and 2000s) to observe the evolution of the coating morphology. Additionally, a fourth sample was deposited at 10 mA cm^{-2} for 4000 s in order to assess the possibility of achieving thicker coatings (Fig. g–h). As it can be observed, the deposit obtained at 5 mA cm^{-2} for 500 s presents a mostly smooth surface, along with some nodular particles with diameters in the order of the hundreds of nanometers. AFM measurements in Fig. 3b accentuate the topography of the surface, revealing the height of the nodules which never exceeds 400 nm. Increasing the deposition time from 500 s to 1000s and 2000s (Fig. 3c–f) does not significantly alter the morphology as the only notable change is a broadening of the nodular particles. At the same time, section images in Fig. 4a and b for selected samples show an extremely homogeneous thickness distribution. It is worth noticing that all the deposits does not reveal any cracks, suggesting that EG-based electrolytes could be promising candidates for high quality thick ruthenium electrodeposition. Indeed, even in the case of deposition at 10 mA cm^{-2} for 4000 s, no cracks could be observed either from the top view (Fig. 3g) or along the section (Fig. 4b). This result is quite remarkable, especially when considering the thickness of the film which is estimated to be 2.35 μm from the section image (Fig. 4b), which is extremely similar to the results obtained by Reddy and Taimsalu [21] with the $[Ru_2(\mu\text{-}N)(H_2O)_2Cl_8]$ aqueous formulation.

An additional set of samples was deposited at current densities of 5, 10 and 20 mA cm^{-2} to observe the changes in the coating thickness as well as provide an estimate of the cathodic efficiency. In this case the total charge density was kept at a constant 5 C cm^{-2} resulting in deposition times of 1000 s, 500 s and 250 s. The thickness of these samples was evaluated from SEM images and the results are shown in Fig. 4c. The ruthenium layer thickness decreases from 317 nm at 5 mA

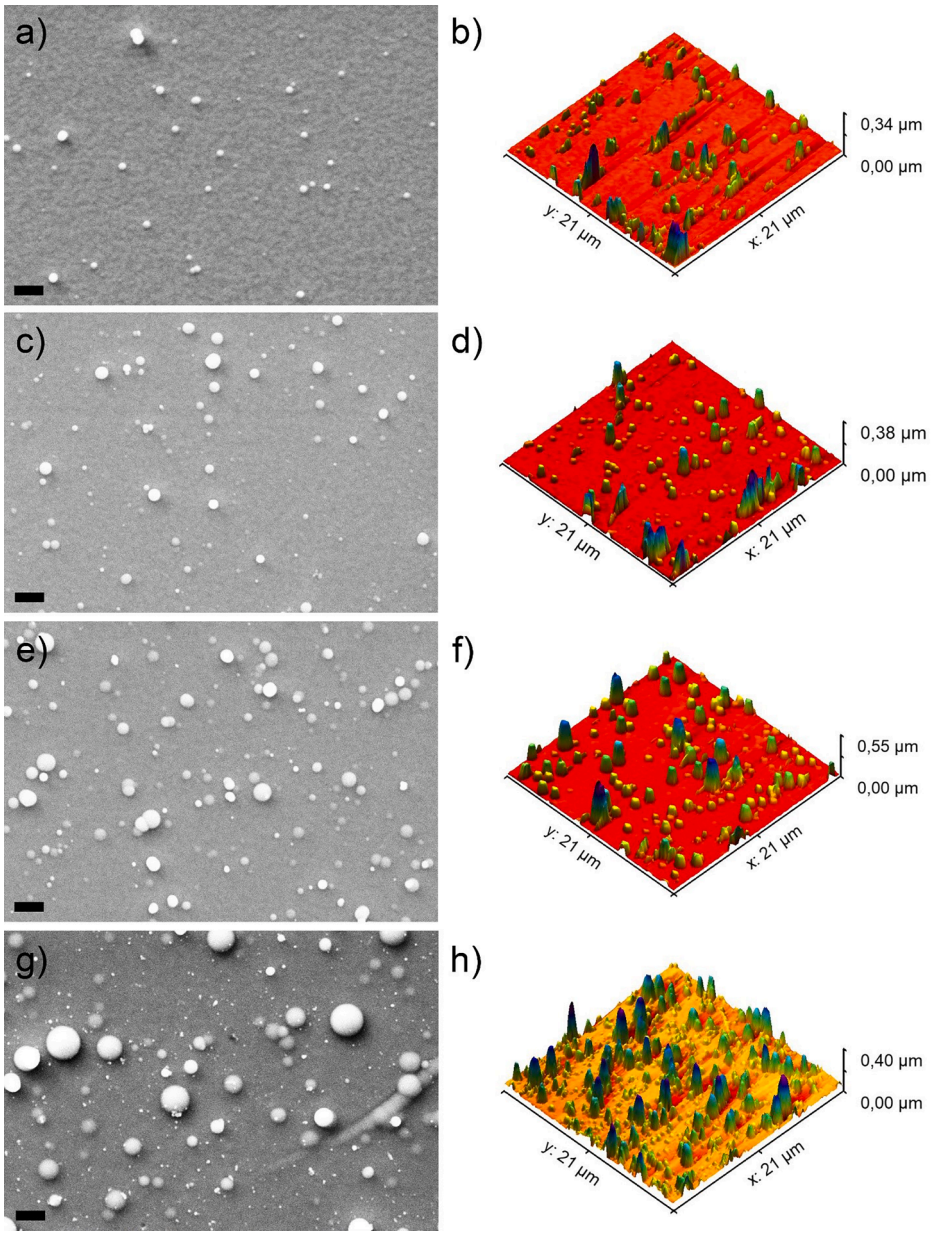

Fig. 3. SEM images and AFM measurements of Ru coatings on Au-sputtered Si wafer at different current density and deposition time. (a) and (b) 5 mA cm^{-2}/500 s, (c) and (d) 5 mA cm^{-2}/1000s, (e) and (f) 5 mA cm^{-2}/2000s, (g) and (h) 10 mA cm^{-2}/4000 s.

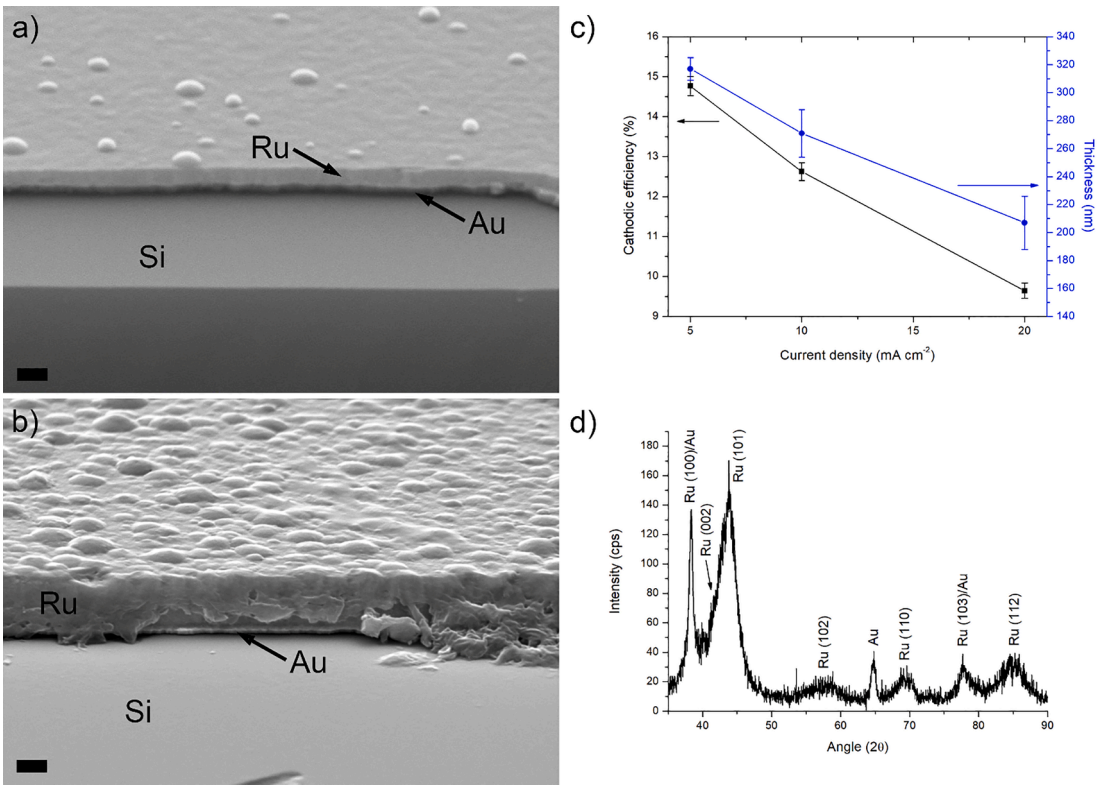

Fig. 4. (a) SEM section of electrodeposited Ru on Au-coated Si wafer obtained at 5 mA cm^{-2} for 1000s (marker size: 500 nm). (b) SEM section of electrodeposited Ru on Au-coated Si wafer obtained at 10 mA cm^{-2} for 4000 s (marker size: 1 μm). (c) Cathodic efficiency and resulting thickness for Ru electrodeposition in EG as a function of the applied current density. (d) XRD of electrodeposited Ru on Au-coated Si wafer obtained at 10 mA cm^{-2} for 4000 s.

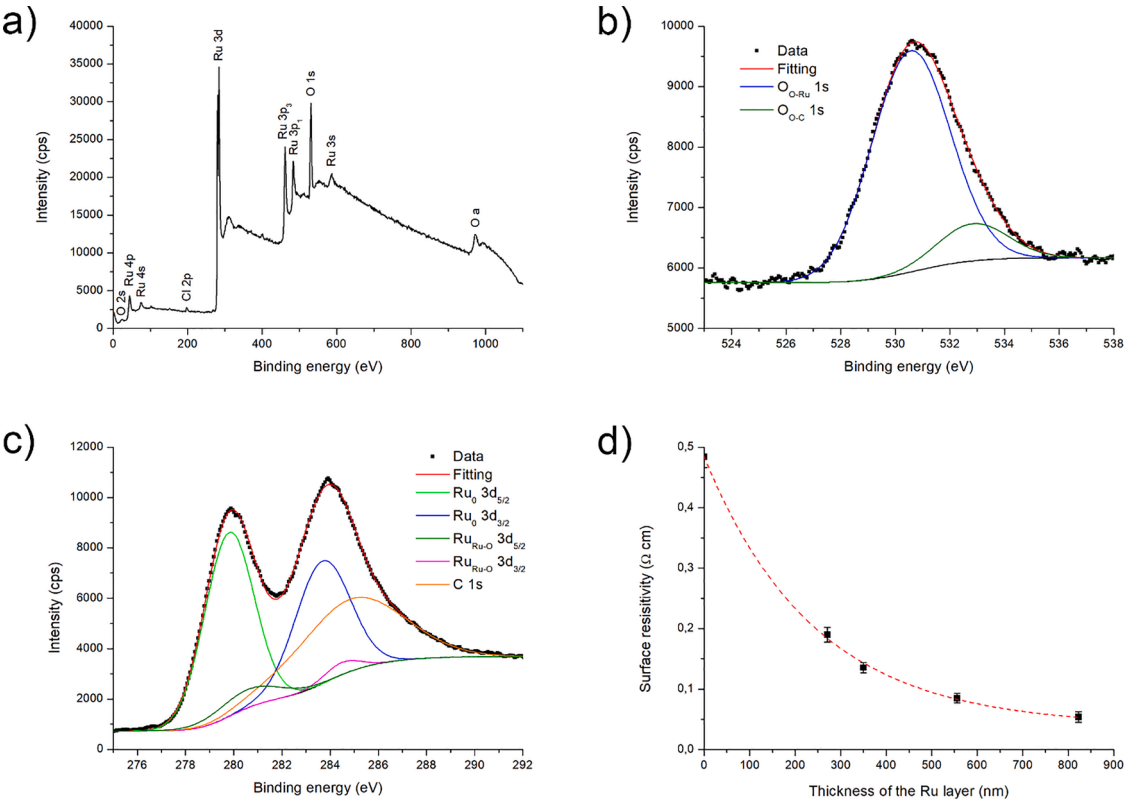

Fig. 5. (a) XPS survey spectra of electrodeposited Ru on Au-coated Si wafer. (b) High resolution scan of Ru 3d peak. (c) High resolution scan of O 1 s peak. (d) Surface resistivity vs. thickness of the Ru on Au-coated Si wafer electrodeposited at different deposition times.

cm^{-2} to 271 nm at 10 mA cm^{-2} and 207 nm at 20 mA cm^{-2}. These results imply a higher deposition rate at lower current density. Indeed, by considering the bulk density of Ru as 12.4 g cm^{-3}, it's possible to estimate the cathodic efficiency of the deposition, which ranges between 9.6% and 14.8%. This low efficiency suggests that ruthenium reduction to the metallic state is accompanied by a secondary reaction, possibly EG deprotonation.

Aside from the peaks from the Au substrate, the XRD spectra of the sample obtained at 10 mA cm^{-2} for 4000 s (Fig. 4d) shows several peaks associated to metallic ruthenium. In particular, the diffractogram matches an hcp lattice, belonging to the P63/mmc spatial group [54] (ICSD #54,236). The relatively broad peaks indicate that the coating could be nanocrystalline. Interestingly, the XRD analysis does not show any trace of oxides or hydroxides, which could sometimes be encountered in Ru electrodeposition from aqueous solvents [24].

In order to gain further insights on the film chemical composition, XPS analysis was carried out. The results of the initial survey are shown in Fig. 5a, where it's possible to distinguish peaks associated to Ru, O and Cl. The high resolution scan of the Ru 3d peak shown in Fig. 5b reveals a doublet due to spin orbit splitting with the two peaks at 279.9 eV and 284.0 eV being respectively associated to the Ru $3d_{5/2}$ and Ru $3d_{3/2}$ [55]. Due to overlapping of the Ru $3d_{3/2}$ and C 1 s peaks, identification of the nature of ruthenium phases is based purely on Ru $3d_{5/2}$ peak [25]. Moreover, this also makes estimation of carbon impurities in the deposit through peak integration rather unreliable. Deconvolution of the Ru $3d_{5/2}$ peak shows that a wide portion of the signal derives from Ru(0), thus confirming the possibility of producing high quality coatings with very few oxide impurities from EG electrolytes. The other peak at higher binding energy is most likely associated to RuO_2 [56,57], which could be formed either during the deposition process or by oxidation through exposure to the atmosphere.

Indeed, the high resolution scan of the O 1 s peak at 530.6 eV in Fig. 5c shows that the majority of oxygen present in the coating is bound to ruthenium and only a small fraction derives from O—C bonds, which could be due to incorporation of EG in the deposit. Integration of the O 1 s peak results in an oxygen content of 9.054% at. Similarly, the Cl content obtained from the integration of the Cl 2p peak (not shown in the figure) is only 0.582% at. Overall, these findings suggest that electrodeposition from EG may serve as a feasible approach to obtain high purity ruthenium coatings.

3.4. Electrical properties of the ruthenium layers

Considering its possible use in a large number of electrical and electronic applications, it is worth characterizing the layers obtained from the electrical point of view. To do this, 4-point probe measurements were carried out on the gold sputtered substrate and on ruthenium layers presenting the following thickness values: 271, 350, 556 and 823 nm. Fig. 5d reports the results obtained in terms of surface resistivity, with only the thickness of the ruthenium layer indicated. Since the ruthenium layers were deposited on the gold sputtered substrate, the final measured value of surface resistivity resulted from the combination of a 100 nm gold layer with layers of ruthenium having the values visible in the figure.

As expected, the values of sheet resistance progressively decreased when the thickness of the ruthenium layer increased. The values of surface resistivity observed are comparable with the values typically measured in the case of Ta barrier layers [58], suggesting that the ruthenium layers plated in the non-aqueous electrolyte hereby described may be potentially suitable as barrier layers for the realization of Cu interconnects [3]. In addition, ruthenium can be employed also to manufacture the interconnect itself. Cu replacement with a high melting metal like Ru can result advantageous in the case of ultra-small interconnects [3].

4. Conclusions

In this work we demonstrated the possibility of using ethylene glycol as electrolyte for the electrodeposition of high purity metallic ruthenium coatings. The presence of ascorbic acid as a reducing agent was demonstrated to be fundamental in enabling the deposition. From UV-visible spectroscopy and cyclic voltammetries, we speculate that the presence of ascorbic acid might lead to a change in ruthenium solvation shell and oxidation state, from +3 to +2. The resulting electrolyte contained a fraction of Ru(II), which resulted stable over time. The coatings obtained with the EG-based electrolyte appeared compact, homogeneous and did not show any cracking up to thicknesses of 2.35 μm, a result that stands out when compared to existing literature on aqueous electrolytes. Furthermore, as a consequence of using a completely water-free electrolyte, the obtained ruthenium films presented a reduced content of oxygen impurities (as demonstrated by XRD and XPS analysis). These results, corroborated by the intrinsic low toxicity and price of the electrolyte, render ethylene glycol an ideal candidate to replace aqueous systems for ruthenium electroplating. This opportunity may possibly enhance the applicability of ruthenium electrodeposition to advanced processes like barrier layers deposition or electronic interconnects microfabrication.

CRediT authorship contribution statement

Federico Lissandrello: Methodology, Investigation, Data curation, Validation, Writing – original draft, Writing – review & editing. **Roberto Bernasconi:** Conceptualization, Methodology, Investigation, Data curation, Writing – original draft, Writing – review & editing. **Claudia Letizia Bianchi:** Investigation, Resources. **Gianmarco Griffini:** Investigation, Resources. **Luca Magagnin:** Validation, Resources, Supervision.

Declaration of Competing Interest

The authors declare that they have no known competing financial interests or personal relationships that could have appeared to influence the work reported in this paper.

Data availability

Data will be made available on request.

Supplementary materials

Supplementary material associated with this article can be found, in the online version, at doi:10.1016/j.electacta.2023.143186.

References

[1] R.L. Graham, G.B. Alers, T. Mountsier, N. Shamma, S. Dhuey, S. Cabrini, R.H. Geiss, D.T. Read, S. Peddeti, Resistivity dominated by surface scattering in sub-50nm Cu wires, Appl. Phys. Lett. 96 (2010), 042116, https://doi.org/10.1063/1.3292022.
[2] J.H. Moon, S. Kim, T. Kim, Y.S. Jeon, Y. Kim, J.P. Ahn, Y.K. Kim, Electrical resistivity evolution in electrodeposited Ru and Ru-Co nanowires, J. Mater. Sci. Technol. 105 (2022) 17–25, https://doi.org/10.1016/j.jmst.2021.06.073.
[3] R. Bernasconi, L. Magagnin, Review—ruthenium as diffusion barrier layer in electronic interconnects: current literature with a focus on electrochemical deposition methods, J. Electrochem. Soc. 166 (2019) D3219–D3225, https://doi.org/10.1149/2.0281901jes.
[4] Y.S. Kim, H. Il Kim, J.H. Cho, H.K. Seo, G.S. Kim, S.G. Ansari, G. Khang, J. J. Senkevich, H.S. Shin, Electrochemical deposition of copper and ruthenium on titanium, Electrochim. Acta 51 (2006) 5445–5451, https://doi.org/10.1016/j.electacta.2006.02.016.
[5] J.J. Tan, X.P. Qu, Q. Xie, Y. Zhou, G.P. Ru, The properties of Ru on Ta-based barriers, Thin Solid Films 504 (2006) 231–234, https://doi.org/10.1016/j.tsf.2005.09.129.
[6] B. Im, S. Kim, S.H. Kim, Nucleation-controlled growth of Cu thin films electrodeposited directly on ALD Ru diffusion barrier in additive-free electrolyte

for Cu interconnect, Microelectron. Eng. 275 (2023), 111991, https://doi.org/10.1016/j.mee.2023.111991.
[7] K. Kugler, M. Luhn, J.A. Schramm, K. Rahimi, M. Wessling, Galvanic deposition of Rh and Ru on randomly structured Ti felts for the electrochemical NH_3 synthesis, Phys. Chem. Chem. Phys. 17 (2015) 3768–3782, https://doi.org/10.1039/C4CP05501B.
[8] I. Lucentini, A. Casanovas, J. Llorca, Catalytic ammonia decomposition for hydrogen production on Ni, Ru and Ni Ru supported on CeO_2, Int. J. Hydrog. Energy 44 (2019) 12693–12707, https://doi.org/10.1016/j.ijhydene.2019.01.154.
[9] M.I. Awad, W.S. Al-Saidi, M.S. El-Deab, B.A. Al-Jahdaly, M.A. Kassem, Enhanced electro-oxidation of methanol at nanoparticle-based Ru/Pt bimetallic catalyst: impact of GC substrate pretreatment, Int. J. Hydrog. Energy 45 (2020) 27171–27181, https://doi.org/10.1016/j.ijhydene.2020.07.056.
[10] Y. Takagi, K. Kerman, C. Ko, S. Ramanathan, Operational characteristics of thin film solid oxide fuel cells with ruthenium anode in natural gas, J. Power Sources 243 (2013) 1–9, https://doi.org/10.1016/j.jpowsour.2013.06.002.
[11] T. Kohma, D. Oyamatsu, S. Kuwabata, Preparation of selective micro glucose sensor without permselective membrane by electrochemical deposition of ruthenium and glucose oxidase, Electrochem. Commun. 9 (2007) 1012–1016, https://doi.org/10.1016/j.elecom.2006.12.015.
[12] R. Hallaj, N. Mohammadian, S. Ghaderi, A. Navaee, Nonenzymatic and low potential glucose sensor based on electrodeposited Ru-nanofilm from ionic liquid electrolyte, Mater. Sci. Eng. B 261 (2020), 114666, https://doi.org/10.1016/J.MSEB.2020.114666.
[13] D.C. Perng, K.C. Hsu, S.W. Tsai, J.B Yeh, Thermal and electrical properties of PVD Ru(P) film as Cu diffusion barrier, Microelectron. Eng. 87 (2010) 365–369, https://doi.org/10.1016/j.mee.2009.06.007.
[14] T.P. Moffat, M. Walker, P.J. Chen, J.E. Bonevich, W.F. Egelhoff, L. Richter, C. Witt, T. Aaltonen, M. Ritala, M. Leskelä, D. Josell, Electrodeposition of Cu on Ru barrier layers for damascene processing, J. Electrochem. Soc. 153 (2006) C37, https://doi.org/10.1149/1.2131826.
[15] H. Wojcik, M. Junige, W. Bartha, M. Albert, V. Neumann, U. Merkel, A. Peeva, J. Gluch, S. Menzel, F. Munnik, R. Liske, D. Utess, I. Richter, C. Klein, H. J. Engelmann, P. Ho, C. Hossbach, C. Wenzel, Physical characterization of PECVD and PEALD Ru(-C) films and comparison with PVD ruthenium film properties, J. Electrochem. Soc. 159 (2011) H166–H176, https://doi.org/10.1149/2.066202jes.
[16] H. Li, D.B. Farmer, R.G. Gordon, Y. Lin, J. Vlassak, Vapor deposition of ruthenium from an amidinate precursor, J. Electrochem. Soc. 154 (2007) D642, https://doi.org/10.1149/1.2789294.
[17] M.J. Parnian, A.A. Khodadadi, A. Taheri Najafabadi, Y. Mortazavi, Preferential chemical vapor deposition of ruthenium on cobalt with highly enhanced activity and selectivity for fischer–tropsch synthesis, Appl. Catal. A Gen. 470 (2014) 221–231, https://doi.org/10.1016/j.apcata.2013.11.004.
[18] T. Aaltonen, P. Alén, M. Ritala, M. Leskelä, Ruthenium thin films grown by atomic layer deposition, Chem. Vap. Depos. 9 (2003) 45–49, https://doi.org/10.1002/cvde.200290007.
[19] C.R.K. Rao, D.C. Trivedi, Chemical and electrochemical depositions of platinum group metals and their applications, Coord. Chem. Rev. 249 (2005) 613–631, https://doi.org/10.1016/j.ccr.2004.08.015.
[20] S.M. Karabanov, O.G. Lokshtanova, A study of the complex composition of sulfamate ruthenium-plating electrolytes, Russ. J. Appl. Chem. 81 (2008) 1000–1003, https://doi.org/10.1134/S1070427208060141.
[21] G.S. Reddy, P. Taimsalu, Electrodeposition of ruthenium, Trans. IMF. 47 (1969) 187–193, https://doi.org/10.1080/00202967.1969.11870111.
[22] F.H. Reid, J.C. Blake, Electrodeposition of ruthenium, Trans. IMF. 38 (1961) 45–51, https://doi.org/10.1080/00202967.1961.11869818.
[23] R. Gusley, Q. Cumston, K.R. Coffey, A.C. West, K. Barmak, Electrodeposition of Ru onto Ru and Au seed layers from solutions of ruthenium nitrosyl sulfate and ruthenium chloride, J. Electrochem. Soc. 168 (2021), 052504, https://doi.org/10.1149/1945-7111/abff68.
[24] D. Kutyła, K. Kołczyk, P. Żabiński, R. Kowalik, A. Kwiecińska, K. Skibinska, Investigation of ruthenium thin layers electrodeposition process under galvanostatic conditions from chloride solutions, Russ. J. Electrochem. 56 (2020) 214–221, https://doi.org/10.1134/S1023193520030064.
[25] D.K. Oppedisano, L.A. Jones, T. Junk, S.K. Bhargava, Ruthenium electrodeposition from aqueous solution at high cathodic overpotential, J. Electrochem. Soc. 161 (2014) D489–D494, https://doi.org/10.1149/2.0441410jes.
[26] M. Pourbaix, Atlas of Electrochemical Equilibria in Aqueous Solutions, 2nd ed., National Association of Corrosion Engineers, 1974. https://books.google.com/books/about/Atlas_of_Electrochemical_Equilibria_in_A.html?hl=it&id=QjxRAAAAMAAJ. accessed June 23, 2023.
[27] R. Zou, Y. Wang, M. Hu, Y. Wei, T. Fujita, Analysis of ruthenium electrodeposition in the nitric acid medium, J. Phys. Chem. C 126 (2022) 4329–4337, https://doi.org/10.1021/acs.jpcc.1c09371.
[28] F. Moyo, J.W. van der Merwe, D. Wamwangi, Corrosion performance of pulse plated ruthenium: dependence on pulse-off time, Surf. Coatings Technol. 307 (2016) 971–977, https://doi.org/10.1016/j.surfcoat.2016.10.016.
[29] J.J. Jow, H.J. Lee, H.R. Chen, M.S. Wu, T.Y. Wei, Anodic, cathodic and cyclic voltammetric deposition of ruthenium oxides from aqueous $RuCl_3$ solutions, Electrochim. Acta 52 (2007) 2625–2633, https://doi.org/10.1016/j.electacta.2006.09.018.
[30] O. Raz, G. Cohn, W. Freyland, O. Mann, Y. Ein-Eli, Ruthenium electrodeposition on silicon from a room-temperature ionic liquid, Electrochim. Acta 54 (2009) 6042–6045, https://doi.org/10.1016/j.electacta.2009.01.012.
[31] M. Jayakumar, K.A. Venkatesan, T.G. Srinivasan, P.R. Vasudeva Rao, Electrochemical behavior of ruthenium (III), rhodium (III) and palladium (II) in 1-butyl-3-methylimidazolium chloride ionic liquid, Electrochim. Acta 54 (2009) 6747–6755, https://doi.org/10.1016/j.electacta.2009.06.043.
[32] O. Mann, W. Freyland, O. Raz, Y. Ein-Eli, Electrochemical deposition of ultrathin ruthenium films on Au(1 1 1) from an ionic liquid, Chem. Phys. Lett. 460 (2008) 178–181, https://doi.org/10.1016/j.cplett.2008.05.096.
[33] G. Kartal Sireli, An investigation of ruthenium coating from LiCl–KCl eutectic melt, Appl. Surf. Sci. 317 (2014) 294–301, https://doi.org/10.1016/j.apsusc.2014.08.116.
[34] W.D. Sides, Q. Huang, Ruthenium electrodeposition from water-in-salt electrolytes and the influence of tetrabutylammonium, J. Electrochem. Soc. 167 (2020), 062509, https://doi.org/10.1149/1945-7111/ab847e.
[35] R. Bernasconi, A. Lucotti, L. Nobili, L. Magagnin, Ruthenium electrodeposition from deep eutectic solvents, J. Electrochem. Soc. 165 (2018) D620–D627, https://doi.org/10.1149/2.0541813jes.
[36] R. Bernasconi, G. Panzeri, G. Firtin, B. Kahyaoglu, L. Nobili, L. Magagnin, Electrodeposition of ZnNi alloys from choline chloride/ethylene glycol deep eutectic solvent and pure ethylene glycol for corrosion protection, J. Phys. Chem. B 124 (2020) 10739–10751, https://doi.org/10.1021/acs.jpcb.0c04784.
[37] G. Panzeri, A. Accogli, E. Gibertini, C. Rinaldi, L. Nobili, L. Magagnin, Electrodeposition of high-purity nanostructured iron films from Fe(II) and Fe(III) non-aqueous solutions based on ethylene glycol, Electrochim. Acta 271 (2018) 576–581, https://doi.org/10.1016/j.electacta.2018.03.174.
[38] T.N. Vorobyova, O.N. Vrublevskaya, Electrochemical deposition of gold–tin alloy from ethylene glycol electrolyte, Surf. Coat. Technol. 204 (2010) 1314–1318, https://doi.org/10.1016/j.surfcoat.2009.10.010.
[39] T.N. Vorobyova, A.A. Kudaka, Electrodeposition of Ni–Sn alloy from ethylene glycol electrolyte. Part 1. Cathodic reactions, Trans. IMF. 100 (2022) 36–42, https://doi.org/10.1080/00202967.2021.2005861.
[40] H. Yamamoto, M. Morishita, Y. Mizuta, A. Masubuchi, Electrodeposition of Co–Sb thermoelectric film from ethylene glycol–$CoCl_2$–$SbCl_3$ solution, Surf. Coatings Technol. 206 (2012) 3415–3420, https://doi.org/10.1016/j.surfcoat.2012.02.027.
[41] X. Yan, H. Liu, K.Y. Liew, Size control of polymer-stabilized ruthenium nanoparticles by polyol reduction, J. Mater. Chem. 11 (2001) 3387–3391, https://doi.org/10.1039/b103046a.
[42] M. Zawadzki, J. Okal, Synthesis and structure characterization of Ru nanoparticles stabilized by PVP or γ-Al_2O_3, Mater. Res. Bull. 43 (2008) 3111–3121, https://doi.org/10.1016/j.materresbull.2007.11.006.
[43] Y. Chen, K.Y. Liew, J. Li, Size-controlled synthesis of Ru nanoparticles by ethylene glycol reduction, Mater. Lett. 62 (2008) 1018–1021, https://doi.org/10.1016/j.matlet.2007.07.038.
[44] J.A. Rard, Chemistry and thermodynamics of ruthenium and some of its inorganic compounds and aqueous species, Chem. Rev. 85 (1985) 1–39, https://doi.org/10.1021/cr00065a001.
[45] G.A. Rechnitz, Preparation of ruthenium(II) by controlled potential reduction, Inorg. Chem. 1 (1962) 953–954, https://doi.org/10.1021/ic50004a058.
[46] M.M.T. Khan, G. Ramachandraiah, R.S. Shukla, Ruthenium(III) chloride in aqueous solution: effects of temperature, ionic strength and solvent isotope on aquation and anation reactions of the chloro complexes, Polyhedron 11 (1992) 3075–3081, https://doi.org/10.1016/S0277-5387(00)80177-1.
[47] M.M.T. Khan, R.S. Shukla, Kinetic and spectroscopic study of the formation of an intermediate ruthenium(III) ascorbate complex in the oxidation of L-ascorbic acid, Polyhedron 10 (1991) 2711–2715, https://doi.org/10.1016/S0277-5387(00)86171-9.
[48] O. Impert, A. Katafias, J. Fenska, M. Chrzanowska, S. Koter, C. Dücker-Benfer, R. van Eldik, Mechanistic complications caused by redox equilibration: ascorbate reduction of a ruthenium(III) complex under low driving force conditions, Eur. J. Inorg. Chem. 2016 (2016) 5380–5386, https://doi.org/10.1002/ejic.201600950.
[49] O. Impert, A. Katafias, M. Chrzanowska, T. Muzioł, G. Wrzeszcz, R. van Eldik, Redox equilibration observed for the reduction of a ruthenium(III) complex by ascorbate under low-driving-force conditions, Eur. J. Inorg. Chem. 2017 (2017) 3275–3284, https://doi.org/10.1002/ejic.201700241.
[50] M.M.T. Khan, R.S. Shukla, Thermodynamics of the homogeneous oxidation of L-ascorbic acid by molecular oxygen catalyzed by ruthenium ion and ruthenium chelates, J. Mol. Catal. 37 (1986) 269–285, https://doi.org/10.1016/0304-5102(86)85016-7.
[51] B.K.K. Kasem, S. Jones, Platinum as a reference electrode in electrochemical measurements, Platin. Met. Rev. 52 (2008) 100–106, https://doi.org/10.1595/147106708X297855.
[52] G. Inzelt, G. Inzelt, A. Lewenstam, F. Scholz, Pseudo-reference electrodes. Handb. Ref. Electrodes, Springer Berlin Heidelberg, Berlin, 2013, pp. 331–332. https://link.springer.com/chapter/10.1007/978-3-642-36188-3_14. accessed June 20, 2023.
[53] I. Mejía-Caballero, T.L. Manh, J. Aldana-González, S.P. Wang, Y.Y. Hsieh, P. Y. Chen, Y. Zhang, D. Poe, L. Heroux, Electrochemical decomposition of primary alcohol groups in deep eutectic solvents, J. Electrochem. Soc. 168 (2021), 106506, https://doi.org/10.1149/1945-7111/AC2D14.
[54] A.V. Morozkin, Y.D. Seropegin, Sm–Ru–Ge system at 1070K, J. Alloys Compd. 365 (2004) 168–172, https://doi.org/10.1016/S0925-8388(03)00652-2.
[55] H.Y.H. Chan, C.G. Takoudis, M.J. Weaver, High-pressure oxidation of ruthenium as probed by surface-enhanced raman and X-ray photoelectron spectroscopies, J. Catal. 172 (1997) 336–345, https://doi.org/10.1006/jcat.1997.1841.

[56] D.J. Morgan, Resolving ruthenium: XPS studies of common ruthenium materials, Surf. Interface Anal. 47 (2015) 1072–1079, https://doi.org/10.1002/sia.5852.
[57] H. Madhavaram, H. Idriss, S. Wendt, Y.D. Kim, M. Knapp, H. Over, J. Aßmann, E. Löffler, M. Muhler, Oxidation reactions over RuO_2: a comparative study of the reactivity of the (110) single crystal and polycrystalline surfaces, J. Catal. 202 (2001) 296–307, https://doi.org/10.1006/jcat.2001.3281.
[58] S.J. Cho, C. Wang, N.Y. Kim, Analysis and optimisation of ohmic contact resistance and surface morphology of a Ta-based diffusion barrier layer in AlGaN/GaN HEMTs on Si (1 1 1) substrates, Solid State Electron. 89 (2013) 85–92, https://doi.org/10.1016/j.sse.2013.07.006.